

This article is licensed under a Creative Commons Attribution-NonCommercial NoDerivatives 4.0 International License.

# Long Noncoding RNA LINC01703 Exacerbates the Malignant Properties of Non-Small Cell Lung Cancer by Upregulating MACC1 in a MicroRNA-605-3p-Mediated Manner

Ziyi Wang,\* Xinyu Zhang,\* Xuedong Zhang,† Xuedong Jiang,‡ and Wenya Li\*

\*Department of Thoracic Surgery, The First Hospital of China Medical University, Shenyang, P.R. China

†Department of Thoracic Surgery, The Sixth People's Hospital of Nantong, Nantong, P.R. China

‡Department of Thoracic Surgery, Liaoning Provincial Corps Hospital, Chinese People's Armed Police Forces, Shenyang, P.R. China

Long intergenic nonprotein-coding RNA 1703 (LINC01703) has diagnostic significance in lung adenocarcinoma. However, its specific roles in non-small cell lung cancer (NSCLC) and downstream mechanisms have not been investigated. In the current study, we characterized the role of LINC01703 in NSCLC malignancy and elucidated its detailed mechanism of action. LINC01703 expression was measured by qRT-PCR. The regulatory effects of LINC01703 on the malignancy of NSCLC cells were assessed by multiple functional experiments. The targeted interaction was confirmed by RNA immunoprecipitation and luciferase reporter assays. Herein, overexpression of LINC01703 in NSCLC was indicated in the TCGA database and further proven in our cohort. Functional studies revealed that knocking down LINC01703 repressed cell proliferation, colony formation, migration, and invasion in vitro, which was accompanied by the induction of apoptosis. The tumor growth of LINC01703-silenced cells was also inhibited in vivo. Mechanistic analyses revealed that LINC01703 functioned as a competing endogenous RNA for microRNA-605-3p (miR-605-3p) in NSCLC cells, which thereby upregulated the miR-605-3p target metastasis associated with colon cancer 1 (MACC1). Rescue experiments highlighted that the regulatory actions of LINC01703 ablation on NSCLC cells were abolished in response to miR-605-3p downregulation or MACC1 overexpression. In conclusion, LINC01703 enhanced the aggressiveness of NSCLC cells by altering miR-605-3p/MACC1. Our work suggests the therapeutic potential of LINC01703/miR-605-3p/MACC1 in NSCLC.

**Key words:** Non-small cell lung cancer (NSCLC); Long noncoding RNAs (lncRNAs); Competing endogenous RNA (ceRNA) model; Therapeutic target

## INTRODUCTION

Lung cancer is the most common human cancer and ranks as the leading cause of tumor-associated death globally<sup>1</sup>. Approximately 2.1 million new lung cancer patients are diagnosed annually, with over 1.8 million deaths<sup>2</sup>. The most common lung cancer subtype is non-small cell lung cancer (NSCLC), which accounts for approximately 80% of all lung cancer cases<sup>3</sup>. NSCLC is highly aggressive, and local or distant metastasis easily occurs at an advanced stage<sup>4</sup>. Currently, surgical excision is regarded as the optimal treatment for NSCLC at an early stage; however, many patients progress to the terminal phase, while they are symptomatic and miss the opportunity for the best therapeutic options<sup>5</sup>. The strategies for diagnosing and

managing NSCLC are constantly progressing; however, the clinical outcomes are still poor, with a 5-year survival rate under 15%<sup>6</sup>. Thus, scientists should investigate the pathogenesis of NSCLC progression in detail, which may facilitate the discovery of novel antitumor therapies.

Although noncoding RNAs lack the ability to encode, they execute regulatory actions on gene expression in different ways<sup>7</sup>. Long noncoding RNAs (lncRNAs) are untranslated transcript molecules that comprise more than 200 nucleotides<sup>8</sup>. Aberrantly expressed lncRNAs have been observed in many pathologies<sup>9</sup>. In cancer research, dysregulated lncRNAs have been identified in nearly all cancer types and are strongly correlated with cancer genesis and progression<sup>10</sup>. Numerous lncRNAs are abnormally expressed in NSCLC and affect aggressive

Address correspondence to Wenya Li, Department of Thoracic Surgery, The First Hospital of China Medical University, No. 155 Nanjing North Road, Shenyang 110001, P.R. China. E-mail: [wenyali@cmu.edu.cn](mailto:wenyali@cmu.edu.cn)

properties by exhibiting pro-oncogenic or anti-oncogenic activity<sup>11</sup>.

MicroRNAs (miRNAs) are named for their transcriptional length of approximately 17–24 nucleotides and lack protein-coding ability<sup>12</sup>. They can suppress gene expression by degrading mRNAs or lowering translation, and regulatory activities occur by binding directly to the 3′-untranslated region (3′-UTR) of mRNA targets<sup>13</sup>. Differentially expressed miRNAs may lead to aberrant expression of disease-associated genes, thereby participating in tumorigenesis and tumor progression<sup>14</sup>. The recent competing endogenous RNA (ceRNA) theory offers a novel mechanism for the direct interaction between lncRNAs and miRNAs<sup>15</sup>. lncRNAs can adsorb miRNAs as ceRNAs and thus weaken the miRNA-induced negative control on their target mRNAs, consequently regulating the aggressive properties of NSCLC cells<sup>16,17</sup>. Therefore, lncRNAs and miRNAs are expected to be effective targets in managing NSCLC.

LINC01703 presented diagnostic significance in lung adenocarcinoma (LUAD)<sup>18</sup>. However, its specific role in NSCLC and the related downstream mechanisms are unknown. As a result, we attempted to determine the expression profile, clinical value, and specific functions of LINC01703 in NSCLC and to clarify the underlying mechanisms used by LINC01703.

## MATERIALS AND METHODS

### *Research Subjects*

Our current research was approved by the Ethics Committee of The First Hospital of China Medical University, which was carried out following the Declaration of Helsinki. All research subjects provided signed informed consent. NSCLC tissues and adjacent normal tissues were acquired from 57 patients in our hospital and stored in liquid nitrogen. The inclusion criteria were as follows: i) diagnosed with NSCLC; ii) had not received radiotherapy, chemotherapy, or other types of anticancer treatments; and iii) agreed to participate in the research. The exclusion criteria included patients with other clinical disorders; patients who received chemotherapy, radiotherapy, or targeted therapies; and patients who refused to take part in the study.

### *Cell Lines and Transfection*

Human nontumorigenic bronchial epithelial BEAS-2B cells (ATCC; Manassas, VA, USA) were cultured in bronchial epithelial cell growth medium (Lonza/Clonetics Corporation, Walkersville, MD, USA) with 10% fetal bovine serum (FBS) (Gibco; Thermo Fisher Scientific, Inc., Waltham, MA, USA). SK-MES-1, H460, and A549 cell lines (all from ATCC) were cultured in MEM, F-12K, and RPMI-1640 medium (all from Gibco), which were all supplemented with 10% FBS. The culture medium for H522 (ATCC) was the same as that for H460. Additionally,

1% penicillin–streptomycin solution (Gibco) was used to prevent cell culture contamination. All cells were cultured in a humidified incubator containing 5% CO<sub>2</sub> at 37°C.

The small interfering (si)RNAs targeting LINC01703 (si-LINC01703), negative control siRNA (si-NC), miR-605-3p mimic, miR-605-3p inhibitor (anti-miR-605-3p), miRNA control (miR-NC), and miRNA inhibitor control (anti-NC) were obtained from GenePharma (Shanghai, China). The si-LINC01703#1 sequence was 5′-ACCAAAAAGGAAAAATTATCTTC-3′; the si-LINC01703#2 sequence was 5′-TTCCACTTTCCTCATCTTATAAA-3′; the si-LINC01703#3 sequence was 5′-ATCACCAAAAAGGAAAAATTATC-3′; and the si-NC sequence was 5′-CACGATAAGACAATGTATTT-3′. The MACC1 overexpression plasmid pcDNA3.1-MACC1 (pc-MACC1) was acquired from Sangon Biotech Co., Ltd. (Shanghai, China). NSCLC cells were seeded into six-well plates and cultivated at 37°C with 5% CO<sub>2</sub> before transfection. Transfection of siRNA (100 pmol), miRNA mimic (100 pmol), miRNA inhibitor (100 pmol), or plasmid (4 μg) was realized using Lipofectamine® 2000 (Invitrogen, Carlsbad, CA, USA). The transfection efficiency was affirmed by quantitative reverse transcriptase-polymerase chain reaction (qRT-PCR).

### *qRT-PCR*

TRIzol (Invitrogen) was used for total RNA extraction. Reverse transcription was carried out using a Mir-X miRNA First-Strand Synthesis Kit (TaKaRa, Dalian, China). Next, PCR amplification was achieved to quantify miR-605-3p with a Mir-X miRNA qRT-PCR TB Green® Kit (TaKaRa). U6 served as a reference for miR-605-3p. For the detection of LINC01703 and MACC1, reverse transcription was conducted with a PrimeScript™ RT reagent kit using gDNA Eraser (TaKaRa). Subsequently, TB Green® Premix Ex Taq™ II (TaKaRa) was employed for quantitative PCR. LINC01703 and MACC1 expression levels were normalized to GAPDH. Gene expression was analyzed by means of the 2<sup>-ΔΔC<sub>q</sub></sup> method<sup>19</sup>. The sequences of the primers are shown in Table 1.

### *Cell Counting Kit-8 (CCK-8) Assay*

After 24 h of incubation, a 100-μl suspension containing 2 × 10<sup>3</sup> transfected cells was added to 96-well plates. Cell proliferation was tested every day until day 3. At the indicated times, 10 μl of CCK-8 solution (Dojindo, Kumamoto, Japan) was applied to the cells followed by 2-h cultivation at 37°C. Next, the absorbance value at 450 nm wavelength was measured by a microplate reader, and the collected data were used to plot growth curves.

### *Colony Formation Assay*

Transfected cells were harvested at 24 h posttransfection. A total of 1 × 10<sup>3</sup> cells were suspended in 2 ml of

**Table 1.** Primer Sequences Used for Quantitative Reverse Transcriptase-Polymerase Chain Reaction (qRT-PCR)

Gene	Sequence (5'-3')
Long intergenic nonprotein-coding RNA 1703 (LINC01703)	Forward: CACAGGCTGGCAAATGGAA Reverse: TGCTGGTGTCATTGAGAACCAG
Metastasis associated with colon cancer 1 (MACC1)	Forward: GGAAGCAGGTGAAGTAGTTCATCA Reverse: GGGTTGGATCAGGAGTAGTGATAGA
GAPDH	Forward: CGGAGTCAACGGATTTGGTCGTAT Reverse: AGCCTTCTCCATGGTGGTGAAGAC
MicroRNA-605-3p (miR-605-3p)	Forward: TCGGCAGGUCUAAAUCUCAUAGU Reverse: CACTCAACTGGTGTCTGTGGA
U6	Forward: CTCGCTTCGGCAGCACA Reverse: AACGCTTCACGAATTTGCGT

complete culture medium, seeded into six-well plates, and cultured under the conditions described above. On day 15, 4% formaldehyde and 0.05% crystal violet (Beyotime, Shanghai, China) were used to fix and stain the colonies, which comprised at least 50 cells. Finally, the colonies were counted under an inverted light microscope (Olympus, Tokyo, Japan).

#### Apoptosis Analyses by Flow Cytometry

Transfected cells were digested with 0.25% trypsin and rinsed with phosphate-buffered saline. The cell pellet was harvested by centrifugation and resuspended in 500  $\mu$ l of binding buffer from an Annexin-V-FITC Apoptosis Detection Kit (KeyGen, Nanjing, China). After double staining with Annexin-V-FITC (5  $\mu$ l) and propidium iodide (5  $\mu$ l) in the dark, early + late apoptosis was measured with a FACScan™ flow cytometer (BD Bioscience, San Jose, CA, USA).

#### Transwell Migration and Invasion Experiments

For the invasion test, Matrigel (BD Bioscience) was evenly spread on the surface of membranes (8  $\mu$ m) of Transwell chambers (Corning Costar, Cambridge, MA, USA), and this step was omitted for migration experiments. After trypsinization, transfected cells were resuspended in FBS-free culture medium. A 200- $\mu$ l cell suspension harboring  $5 \times 10^4$  cells was seeded into the upper compartments, while the lower compartments were covered with 600  $\mu$ l of 20% FBS-supplemented medium. After 24 h of cultivation, noninvaded cells were carefully cleaned with a cotton bud. The cells on the lower side of the membranes were fixed in 100% methanol and stained with 0.05% crystal violet. After taking the photos (200 $\times$  magnification), the number of migrated/invaded cells was counted from a total of five randomly chosen images using an inverted light microscope.

#### Xenograft Tumor Growth Model

All animal experiments were conducted with the permission of the Animal Care Committee of The First Hospital of China Medical University. Short-hairpin RNA (shRNA) to ablate the expression of LINC01703 (sh-LINC01703)

and negative control shRNA (sh-NC) were purchased from GenePharma (Shanghai, China) and inserted into the pLKO.1 vector (Addgene Inc., Watertown, MA, USA). The sh-LINC01703 sequence was 5'-CCGGACCAAAAAGG AAAAATTATCTTCCTCGAGGAAGATAATTTTTCC TTTTGGTTTTTTG-3', and the sh-NC sequence was 5'-CCGGCAGGATAAGACAATGTATTTCTCGAGAAAT ACATTGTCTTATCGTGTTTTTG-3'. The yield vectors alongside psPAX2 and pMD2.G were transfected into 293T cells (National Collection of Authenticated Cell Cultures, Shanghai, China) using Lipofectamine® 2000. After 48 h of cultivation, the lentiviruses carrying either sh-LINC01703 or sh-NC were collected and used to infect A549 cells. Puromycin was utilized to select A549 cells stably over-expressing sh-LINC01703 or sh-NC.

BALB/c male nude mice were acquired from Vital River Laboratory (Beijing, China) at 4–6 weeks of age. A549 cells<sup>20–22</sup> stably transfected with sh-LINC01703 or sh-NC were subcutaneously injected into the flanks of mice. A total of six mice were used, and each group contained three mice. The tumor width and length were recorded weekly with a Vernier caliper. The formula<sup>23–25</sup> volume =  $0.5 \times \text{length} \times \text{width}^2$  was applied for tumor volume determination. All mice were euthanized at 28 days postinjection, and tumor xenografts were stripped for weighing and immunohistochemistry of MACC1, Ki-67 and cleaved caspase 3. Additionally, at 28 days postinjection, the RNA and protein of tumor xenografts were extracted and used for molecular detection.

#### Bioinformatics Analysis

The interaction between LINC01703 and miR-605-3p was predicted using starBase 3.0 (<http://starbase.sysu.edu.cn/>) and miRDB (<http://mirdb.org/>). The putative targets of miR-605-3p were screened out with TargetScan (<http://www.targetscan.org/>) and miRDB.

#### Luciferase Reporter Assay

LINC01703 and MACC1 regions carrying the wild-type (WT) miR-605-3p binding sites were cloned into the psi-CHECK2 luciferase reporter vector (Promega, Madison,

WI, USA), ultimately generating WT-LINC01703 and WT-MACC1 reporter plasmids. The mutant (MUT) reporter plasmids MUT-LINC01703 and MUT-MACC1 were constructed following the same instructions. For the reporter assay, cotransfection of reporter plasmids and miR-605-3p mimic or miR-NC was achieved using Lipofectamine<sup>®</sup> 2000 transfection reagent. After culturing for 48 h, luciferase activity was monitored applying a Dual-Luciferase Reporter Assay system (Promega) following the manufacturer's instructions.

#### *Nuclear/Cytoplasmic Fractionation Assay*

NSCLC cells were lysed to obtain cytoplasmic and nuclear fractions utilizing the Cytoplasmic and Nuclear RNA Purification Kit (Norgen, Thorold, ON, Canada). RNA from cytoplasmic and nuclear lysates was isolated and analyzed by qRT-PCR to assess LINC01703 localization.

#### *RNA Immunoprecipitation (RIP)*

By conducting RIP, we tested the direct interaction between LINC01703, miR-605-3p, and MACC1 using a Magna RIP RNA Binding Protein Immunoprecipitation Kit (Merck Millipore, Darmstadt, Germany). Following lysis in complete RIP lysis buffer, whole cell lysates were harvested and cultivated with RIP buffer supplemented with magnetic beads, which were coupled with anti-Argonaute2 (Ago2) antibody or IgG control (Merck Millipore). After overnight incubation at 4°C, a magnetic separator was used to collect the magnetic beads. The beads were then rinsed with RIP buffer and probed with Proteinase K. The immunoprecipitated RNA was extracted prior to qRT-PCR analysis.

#### *Western Blotting*

Protein lysates were extracted using PMSF-supplemented RIPA lysis buffer and quantified using a BCA kit (both from KeyGen). The same amount of protein was loaded into each lane, and then the proteins were separated by 10% SDS-PAGE and transferred onto PVDF membranes. Next, the membranes were blocked utilizing 5% skim milk and then probed with a primary antibody targeting MACC1 (ab226803; 1:1,000 dilution) or GAPDH (ab181603; 1:1,000 dilution; Abcam, Cambridge, MA, USA) at 4°C overnight. After being rinsed three times, horseradish peroxidase-conjugated goat secondary antibody (ab6721; 1:5,000 dilution; Abcam) was further incubated with the membranes at room temperature for 1 h. Finally, the signals were detected with an ECL detection system (KeyGen).

#### *Immunohistochemistry*

Tumor xenografts were immersed in formalin at 4°C for 24 h and then embedded in paraffin. The sections

were sliced at a thickness of 4 μm, after which they were subjected to dewaxing, rehydration, and heated antigen retrieval. After incubation with a primary antibody targeting MACC1 (ab242199; Abcam) at 4°C overnight, the sections were treated with a secondary antibody (ab205719; Abcam) at room temperature for 30 min. Thereafter, 3,3'-diaminobenzidine tetrahydrochloride and hematoxylin were used for chromogenic revelation and counterstaining, respectively. Finally, the images were observed under a light microscope (Olympus Corporation).

#### *Statistical Analysis*

All experiments were repeated three times, and the acquired data are presented as the mean ± standard deviation. Student's *t*-test was used to compare the difference between two groups. The statistical significance among multiple groups was determined utilizing one-way analysis of variance and Tukey's post hoc test. The Pearson correlation coefficient was used to evaluate the expression correlation. A value of  $p < 0.05$  indicated a statistically significant difference.

## RESULTS

### *Depleted LINC01703 Impedes the Aggressive Properties of NSCLC Cells In Vitro*

To determine the expression profile of LINC01703, we first discovered through The Cancer Genome Atlas (TCGA) database that, compared with normal lung tissues, LINC01703 was overexpressed in lung squamous cell carcinoma (LUSC) and LUAD tissues (Fig. 1A). Next, we assessed the level of LINC01703 expression in 57 pairs of NSCLC tissues and adjacent healthy control tissues. In agreement with the observations from the TCGA database, LINC01703 was obviously upregulated in NSCLC tissues (Fig. 1B).

To investigate the role of LINC01703 in NSCLC, we initially tested LINC01703 expression in NSCLC cell lines. qRT-PCR confirmed that LINC01703 was highly expressed in NSCLC cell lines (Fig. 1C). The SK-MES-1 and A549 cell lines displayed the most noticeable increase in LINC01703 levels and were selected for subsequent experiments. Three siRNAs were designed to specifically deplete LINC01703 levels. si-LINC01703#1 was the most efficient siRNA and was chosen for subsequent loss-of-function assays (Fig. 1D). Through CCK-8 and colony formation assays, we found that LINC01703 ablation evidently impaired the proliferation and colony formation of NSCLC cells (Fig. 1E and F). In addition, downregulation of LINC01703 resulted in an evident enhancement of NSCLC cell apoptosis (Fig. 1G). The migration and invasion (Fig. 1H) of LINC01703-deficient NSCLC cells were strikingly hindered compared with those of the si-NC control. Overall, LINC01703 acts as a tumor-promoting lncRNA in NSCLC.

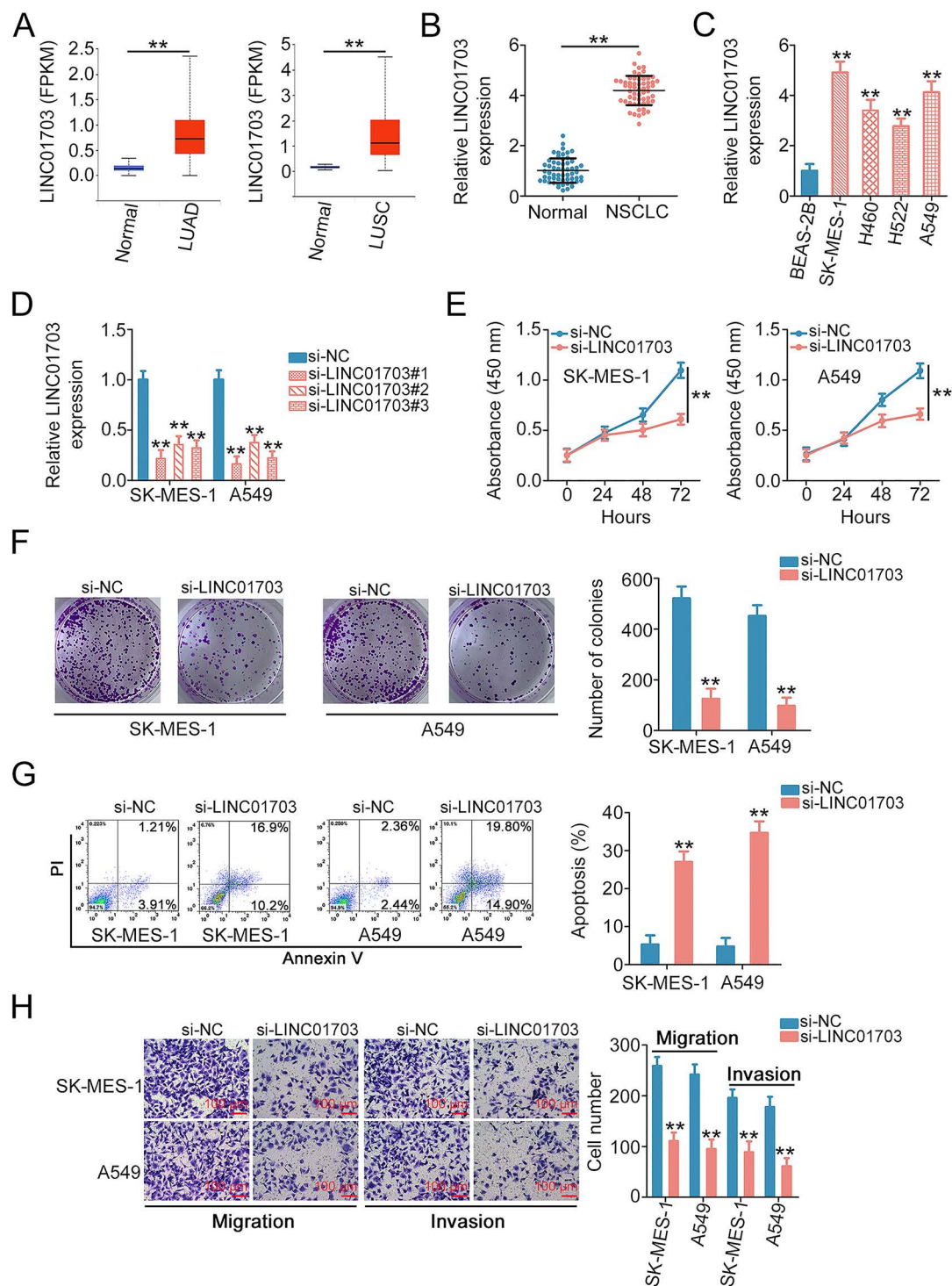


**Figure 1.** Low levels of long intergenic nonprotein-coding RNA 1703 (LINC01703) restrict the malignant properties of non-small cell lung cancer (NSCLC) cells. (A) The Cancer Genome Atlas (TCGA) dataset was utilized to analyze LINC01703 in lung adenocarcinoma (LUAD) and lung squamous cell carcinoma (LUSC). (B) Expression of LINC01703 in NSCLC tissues was detected utilizing quantitative reverse transcriptase-polymerase chain reaction (qRT-PCR). (C) qRT-PCR was conducted to detect LINC01703 in NSCLC cell lines. (D) The interference efficiency of small interfering (si)-LINC01703 in NSCLC cells was assessed using qRT-PCR. (E, F) The proliferation and colony formation of LINC01703-deficient NSCLC cells were tested utilizing Cell Counting Kit-8 (CCK-8) and colony formation assays. (G) Flow cytometry analysis was employed to detect the early+late apoptotic rate in NSCLC cells after LINC01703 silencing. (H) The motility of NSCLC cells after si-LINC01703 transfection were evaluated by Transwell migration and invasion experiments (magnification: 200 $\times$ ). \*\* $p < 0.01$ .

### LINC01703 Acts as an miR-605-3p Sponge in NSCLC

To determine the mechanism by which LINC01703 exacerbates NSCLC oncogenicity, we first determined its subcellular localization and confirmed that LINC01703 is a cytoplasmic lncRNA (Fig. 2A), implying that the

lncRNA is a natural miRNA sponge. By utilizing starBase 3.0 and miRDB, we discovered six overlapping miRNAs and subjected them to further examination (Fig. 2B). We subsequently ablated LINC01703 expression in NSCLC cells and then detected changes in the six

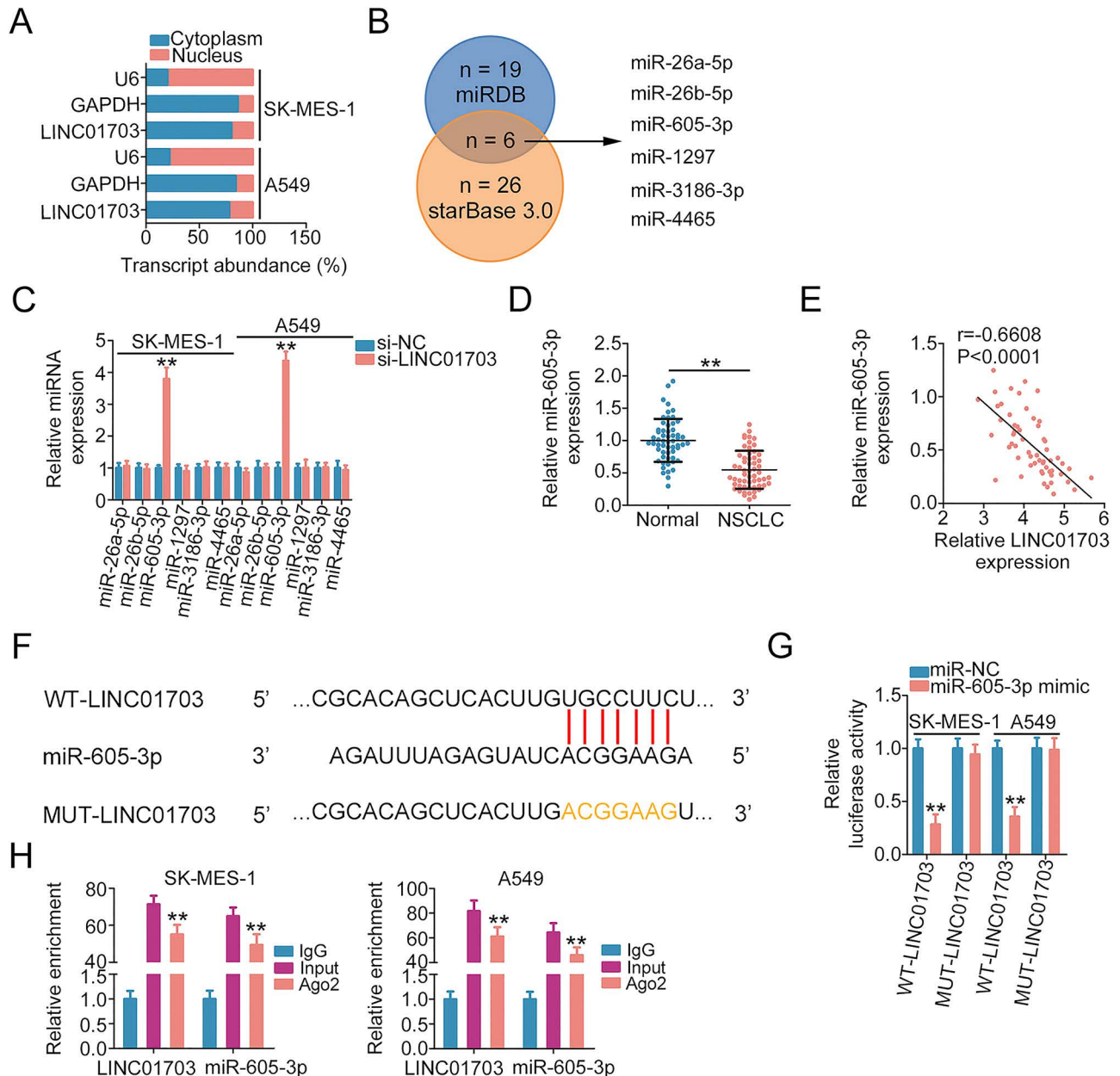


**Figure 2.** LINC01703 acts as a molecular sponge for microRNA-605-3p (miR-605-3p). (A) Nuclear/cytoplasmic fractionation assays characterized the subcellular localization of LINC01703 in NSCLC cells. (B) Overlapping target miRNAs of LINC01703 were predicted by StarBase and miRDB. (C) LINC01703-silenced NSCLC cells were subjected to qRT-PCR to measure miR-26a-5p, miR-26b-5p, miR-3186-3p, miR-605-3p, miR-1297, and miR-4465. (D) Expression of miR-605-3p in NSCLC tissues was detected utilizing qRT-PCR. (E) The expression relationship between LINC01703 and miR-605-3p in NSCLC tissues. (F) The schematic shows the miR-605-3p wild-type (WT) target site within LINC01703 and mutant (MUT) miR-605-3p-binding sequences. (G) A luciferase reporter assay was implemented to reveal the target interaction between LINC01703 and miR-605-3p. (H) RNA immunoprecipitation (RIP) confirmed that LINC01703 and miR-605-3p could be immunoprecipitated with the Argonaute2 (Ago2) antibody.  $**p < 0.01$ .

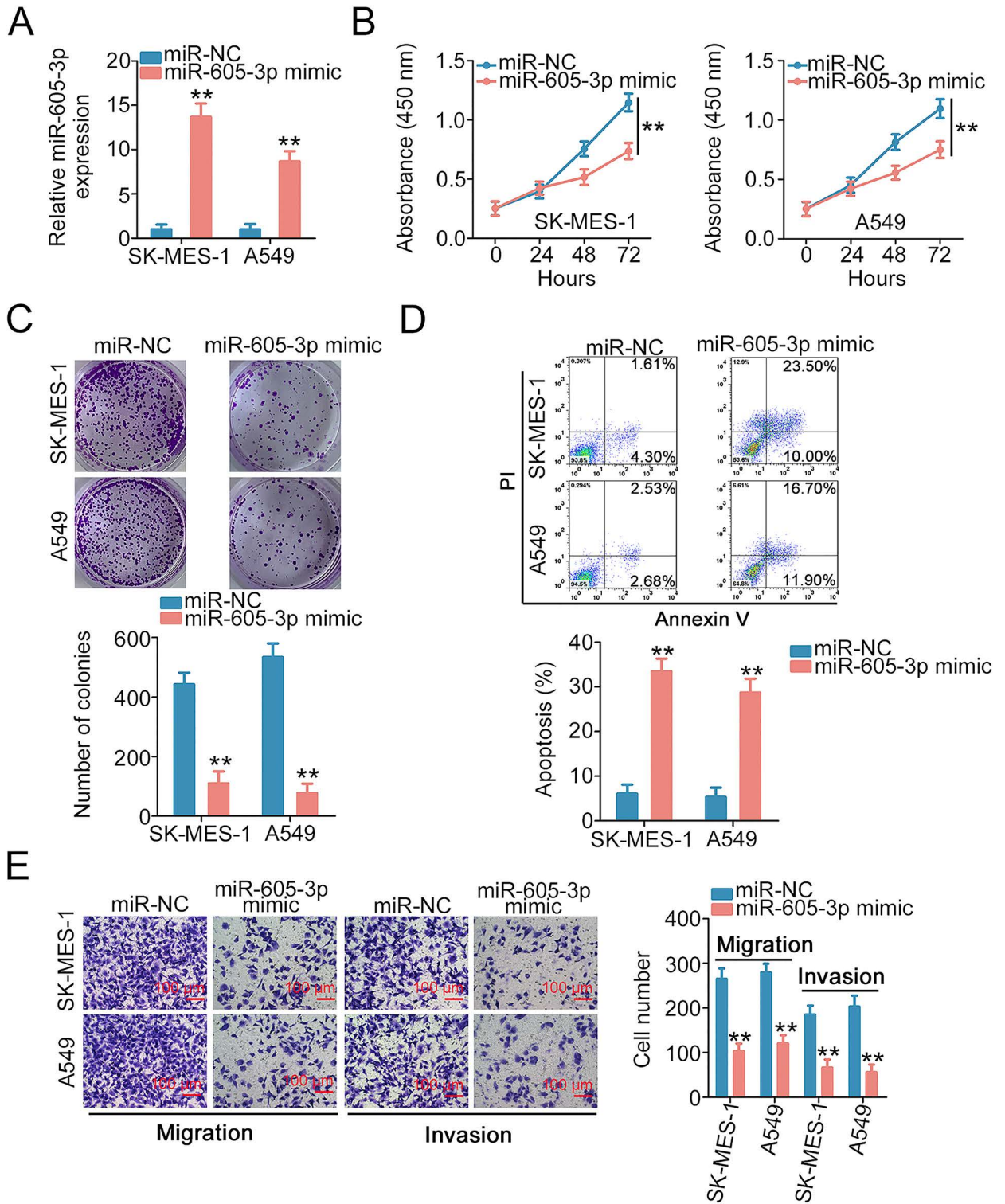


**Figure 3.** miR-605-3p exerts anticarcinogenic effects on NSCLC cells. (A) The efficiency of the miR-605-3p mimic transfection in NSCLC cells. (B, C) After miR-605-3p upregulation, CCK-8 and colony formation assays were employed to assess cell proliferation and colony formation. (D) The early+late apoptosis of miR-605-3p mimic-transfected NSCLC cells was detected using flow cytometry analysis. (E) The migratory and invasive properties were examined in NSCLC cells after miR-605-3p mimic treatment (magnification: 200×). \*\* $p < 0.01$ .

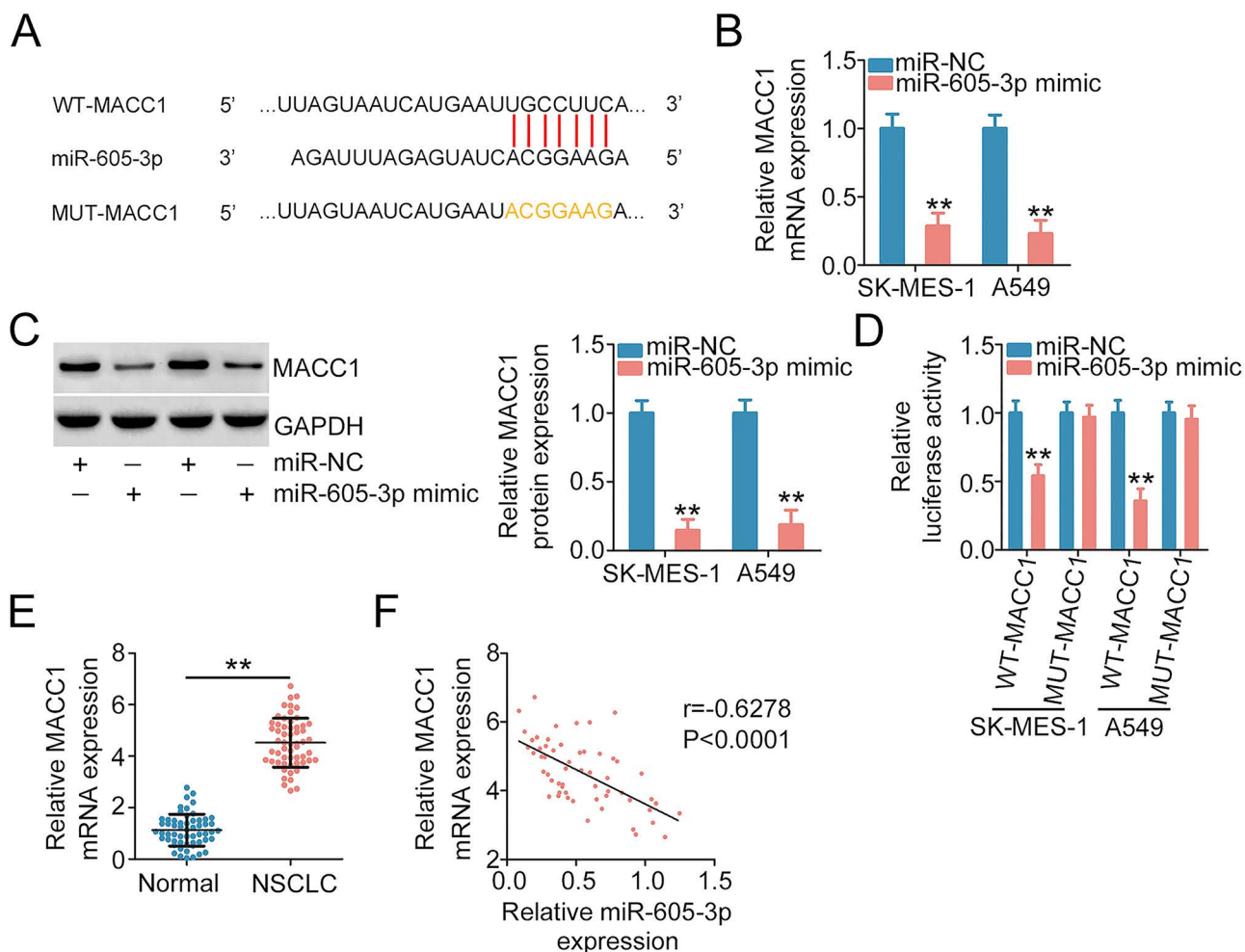
miRNA candidates. As a result, we observed that miR-605-3p was remarkably increased in NSCLC cells upon si-LINC01703 transfection, whereas the others remained relatively unchanged (Fig. 2C). Furthermore, downregulated miR-605-3p was observed in NSCLC tissues (Fig. 2D), which was negatively correlated with LINC01703 levels (Fig. 2E).

Figure 2F shows the conserved binding site of miR-605-3p within LINC01703. A luciferase reporter assay was employed to verify the binding site between miR-605-3p and LINC01703. Ectopic miR-605-3p expression inhibited the luciferase activity of WT-LINC01703, whereas the repressive efficacy was lost after the binding site was mutated (Fig. 2G). Moreover, as shown in RIP experiments, miR-605-3p and LINC01703 were precipitated by the Ago2 antibody (Fig. 2H). Therefore, miR-605-3p is sequestered by LINC01703 in NSCLC.

#### miR-605-3p Directly Targets MACC1 in NSCLC

We increased miR-605-3p expression by transfection with the miR-605-3p mimic construct (Fig. 3A), and then we determined the biological functions of miR-605-3p in NSCLC. Interestingly, miR-605-3p was identified as a tumor-suppressive miRNA in NSCLC cells and participated in regulating cell proliferation, colony formation, and apoptosis (Fig. 3B–D). Additionally, exogenous miR-605-3p hindered the motility (Fig. 3E) of NSCLC cells.

To identify the downstream target of miR-605-3p, we used two online prediction tools and discovered an miR-605-3p target site on MACC1 (Fig. 4A). The luciferase activity of WT-MACC1, but not MUT-MACC1, was decreased by the miR-605-3p mimic construct in NSCLC cells (Fig. 4B). After overexpressing miR-605-3p,



**Figure 4.** miR-605-3p directly targets metastasis associated with colon cancer 1 (MACC1) in NSCLC cells. (A) A schematic is shown of the miR-605-3p WT target site within MACC1 and MUT miR-605-3p-binding sequences. (B, C) MACC1 levels in NSCLC cells when miR-605-3p was upregulated. (D) The targeting relationship between miR-605-3p and MACC1 was proven by luciferase reporter assay. (E) Expression of MACC1 in NSCLC tissues was detected utilizing qRT-PCR. (F) The expression relationship between MACC1 and miR-605-3p in NSCLC tissues.  $**p < 0.01$ .



MACC1 level was clearly decreased in NSCLC cells (Fig. 4C and D). Correlation analysis revealed that highly expressed MACC1 (Fig. 4E) in NSCLC tissues exhibited a negative correlation with miR-605-3p (Fig. 4F). Altogether, miR-605-3p directly targeted MACC1 in NSCLC.

#### *LINC01703 Affects MACC1 Expression Using an miR-605-3p-Mediated Mechanism*

Because of the interactions between LINC01703 and miR-605-3p as well as miR-605-3p and MACC1, we next asked whether LINC01703 was capable of affecting MACC1 expression. Our results illustrated that when LINC01703 was knocked down, MACC1 levels were reduced in NSCLC cells (Fig. 5A and B). However,

miR-605-3p inhibition induced by anti-miR-605-3p counteracted the si-LINC01703-dependent decrease in MACC1 (Fig. 5C and D). Additionally, a positive correlation between LINC01703 and MACC1 was confirmed in NSCLC tissues (Fig. 5E). Furthermore, LINC01703, miR-605-3p, and MACC1 were precipitated with an Ago2 antibody (Fig. 5F). In summary, LINC01703 controls MACC1 expression through an miR-605-3p-mediated mechanism.

#### *Interference With LINC01703 Disrupts the Malignant Properties of NSCLC Cells by Targeting miR-605-3p/MACC1*

Finally, rescue experiments were performed to clarify whether the miR-605-3p/MACC1 axis contributed

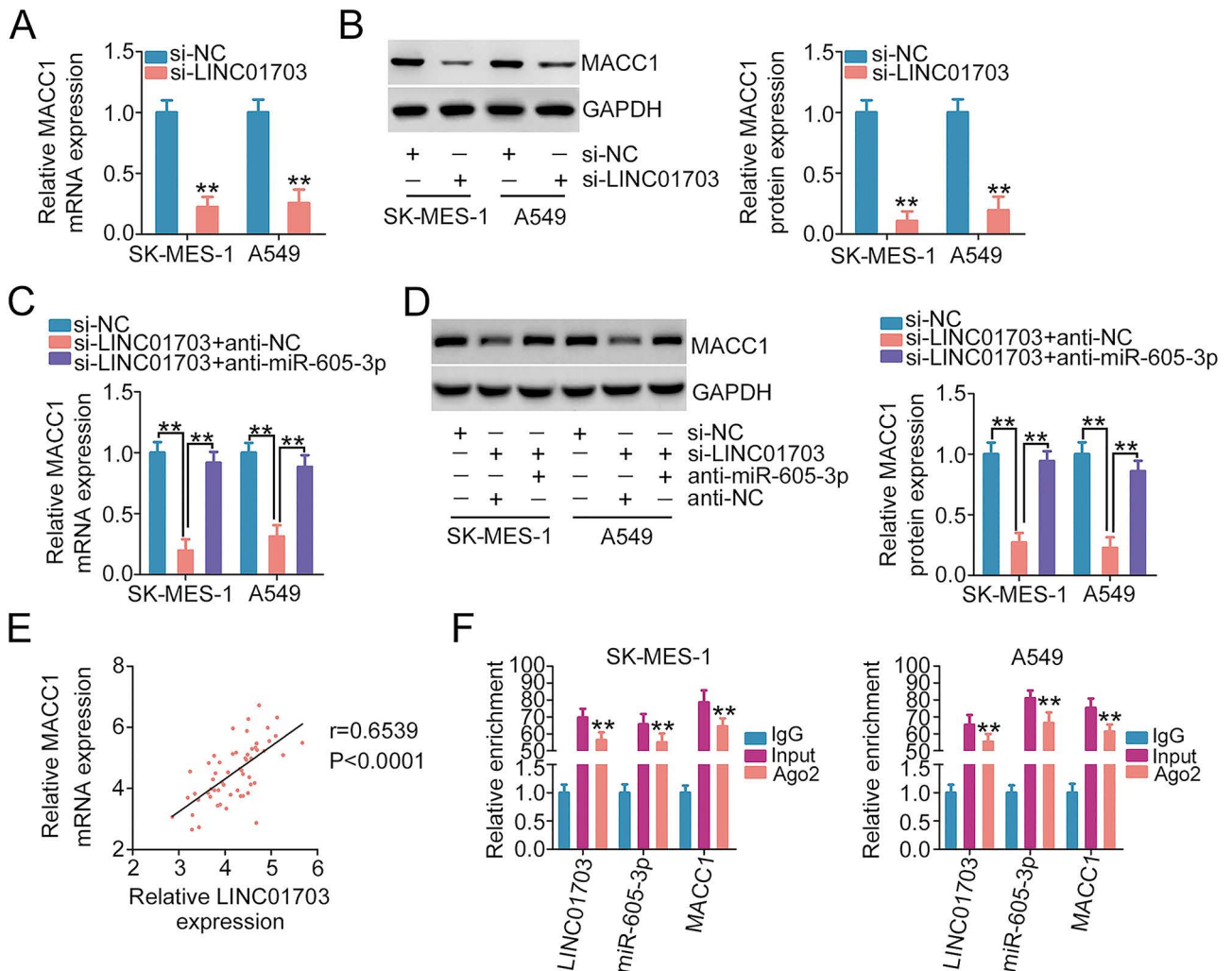


**Figure 5.** LINC01703 antagonizes miR-605-3p, consequently regulating MACC1 in NSCLC. (A, B) MACC1 expression was quantified in LINC01703-depleted NSCLC cells. (C, D) LINC01703-deficient NSCLC cells were further treated with anti-miR-605-3p or anti-NC and subjected to MACC1 quantification. (E) The correlation between MACC1 and LINC01703 levels in NSCLC tissues was uncovered by the Pearson correlation coefficient. (F) RIP confirmed that LINC01703, miR-605-3p, and MACC1 could be immunoprecipitated with the Ago2 antibody. \*\* $p<0.01$ .

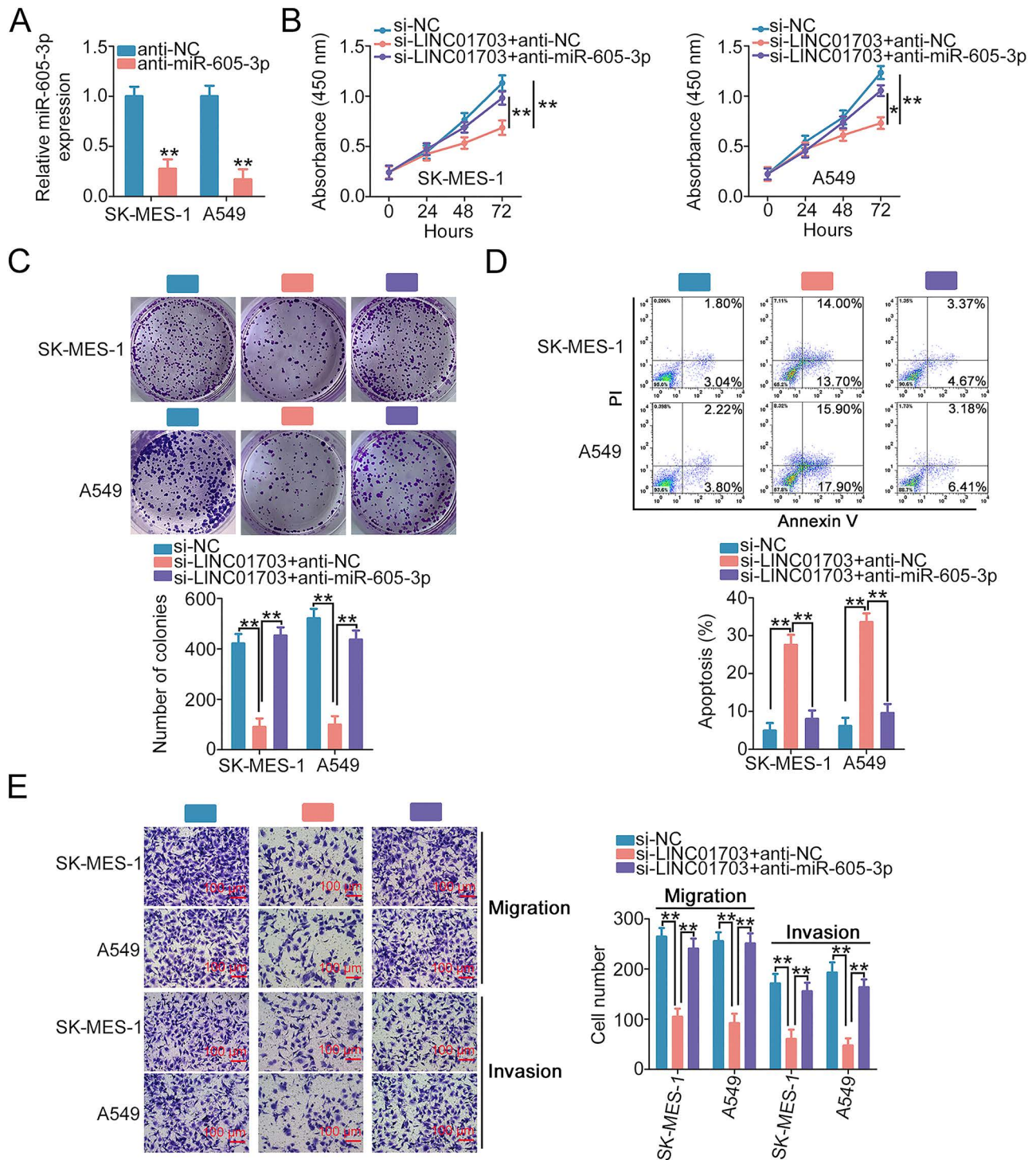


**Figure 6.** Anti-miR-605-3p treatment abrogates the repressive effects of si-LINC01703 in NSCLC cells. (A) The efficiency of anti-miR-605-3p transfection in NSCLC cells. (B–E) Anti-miR-605-3p or anti-NC in parallel with si-LINC01703 was transfected into NSCLC cells, followed by the evaluation of cell proliferation, colony formation, early + late apoptosis, migration, and invasion (magnification: 200×). \* $p < 0.05$  and \*\* $p < 0.01$ .

to the si-LINC01703-mediated inhibition of cancer cell aggressive properties. First, the efficiency of the anti-miR-605-3p transfection was tested by performing qRT-PCR (Fig. 6A). As illustrated in Figure 6B and C, after

treatment with anti-miR-605-3p, the proliferative and colony-forming abilities impaired by si-LINC01703 were almost recovered. In addition, inhibiting miR-605-3p reversed the effects of si-LINC01703 on NSCLC cell

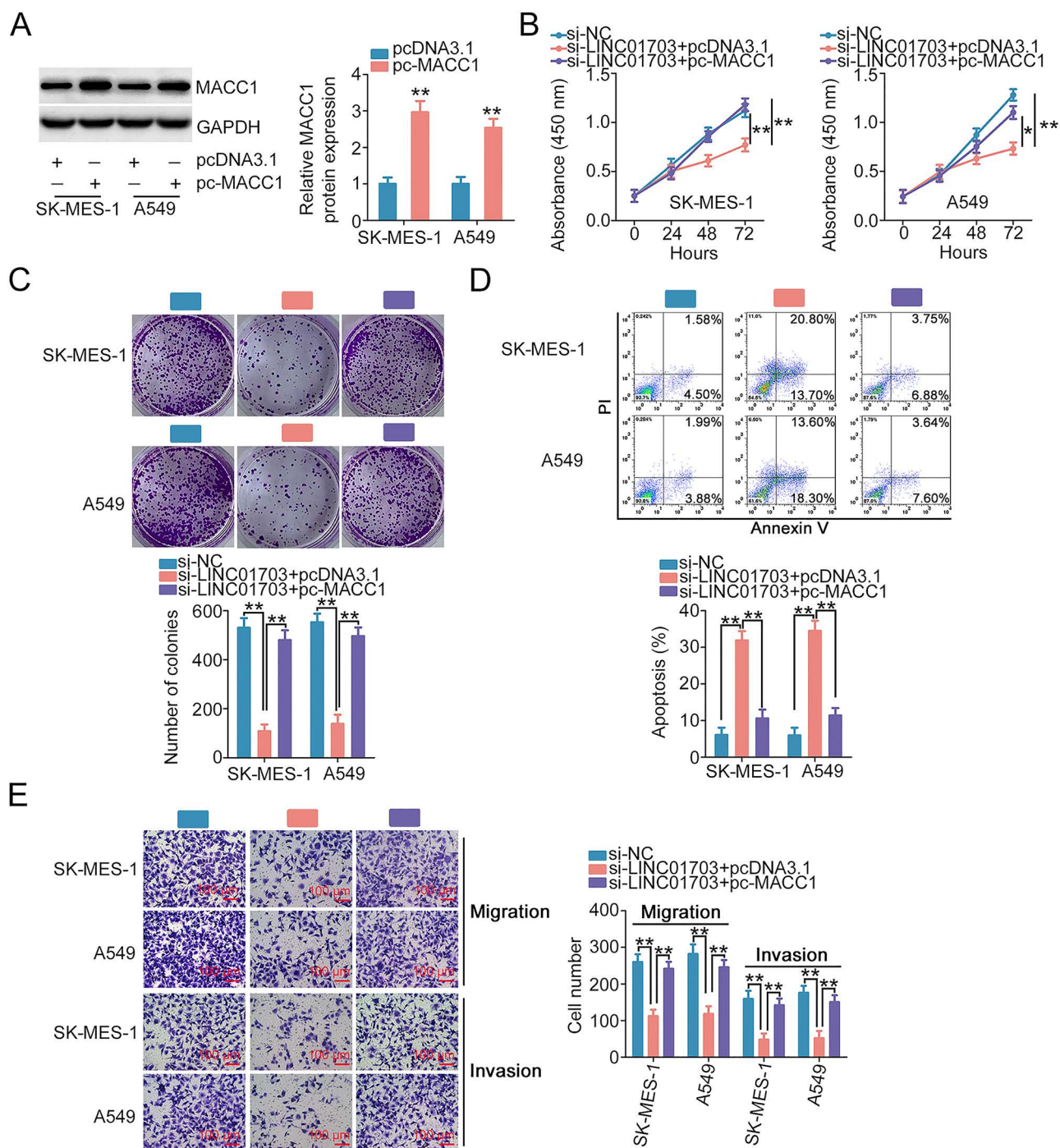


**Figure 7.** The regulatory actions of si-LINC01703 in NSCLC cells are counteracted by pcDNA3.1-MACC1 (pc-MACC1) treatment. (A) Western blotting was used to confirm the efficiency of pc-MACC1 transfection in NSCLC cells. (B–D) After pc-MACC1 or pcDNA3.1 was transfected into LINC01703-silenced NSCLC cells, cell proliferation, colony formation, and early + late apoptosis was assessed. (E) The motility of NSCLC cells treated as described above was unveiled by conducting Transwell migration and invasion experiments (magnification: 200 $\times$ ). \* $p < 0.05$  and \*\* $p < 0.01$ .

apoptosis (Fig. 6D). LINC01703 knockdown resulted in impaired NSCLC cell motility, and this effect was counteracted by anti-miR-605-3p treatment (Fig. 6E).

Western blotting verified that pc-MACC1 transfection led to an increase in MACC1 expression in NSCLC cells (Fig. 7A). The decreased proliferation and colony formation of LINC01703-silenced NSCLC cells was recovered by pc-MACC1 cotransfection (Fig. 7B and C). MACC1 overexpression abrogated the proapoptotic effect of si-LINC01703 on NSCLC cells (Fig. 7D). Furthermore, a decrease in migratory and invasive properties was confirmed in LINC01703-deficient NSCLC cells, but MACC1 reintroduction ameliorated these repressive activities (Fig. 7E). These results indicate that the miR-605-3p/MACC1 axis is activated as the downstream mediator of LINC01703 in NSCLC cells.

#### LINC01703 Deficiency Impedes Tumor Growth In Vivo

A xenograft tumor growth model was established to determine the effect of LINC01703 knockdown on tumor growth in vivo. The volume (Fig. 8A and B) and weight (Fig. 8C) of tumors were suppressed with sh-LINC01703 injection, indicating that depletion of LINC01703 slowed

tumor growth in vivo. To further test the association among LINC01703, miR-605-3p, and MACC1, their expression levels were determined in harvested tumor xenografts. LINC01703 (Fig. 8D) and MACC1 (Fig. 8E) levels were decreased, whereas miR-605-3p was overexpressed (Fig. 8F) in tumors originating from the sh-LINC01703 group. In addition, immunohistochemistry analysis verified that the loss of LINC01703 resulted in reductions in MACC1 and Ki-67 expression and an increase in that of cleaved caspase 3 (Fig. 8G). In short, LINC01703 inhibition suppresses tumor growth in vivo.

## DISCUSSION

Cancer studies have focused on developing effective targets for cancer diagnosis, prognosis and treatment, which may efficiently prolong the lives of patients and increase their quality of life<sup>26-28</sup>. As next-generation sequencing and transcriptomics have progressed, studying the modulatory role of lncRNAs during oncogenesis and cancer progression is a promising research area<sup>29</sup>. Many lncRNAs dysregulated in NSCLC can either delay or accelerate cancer progression<sup>30-32</sup>, indicating that they may be attractive biomarkers for early diagnosis and

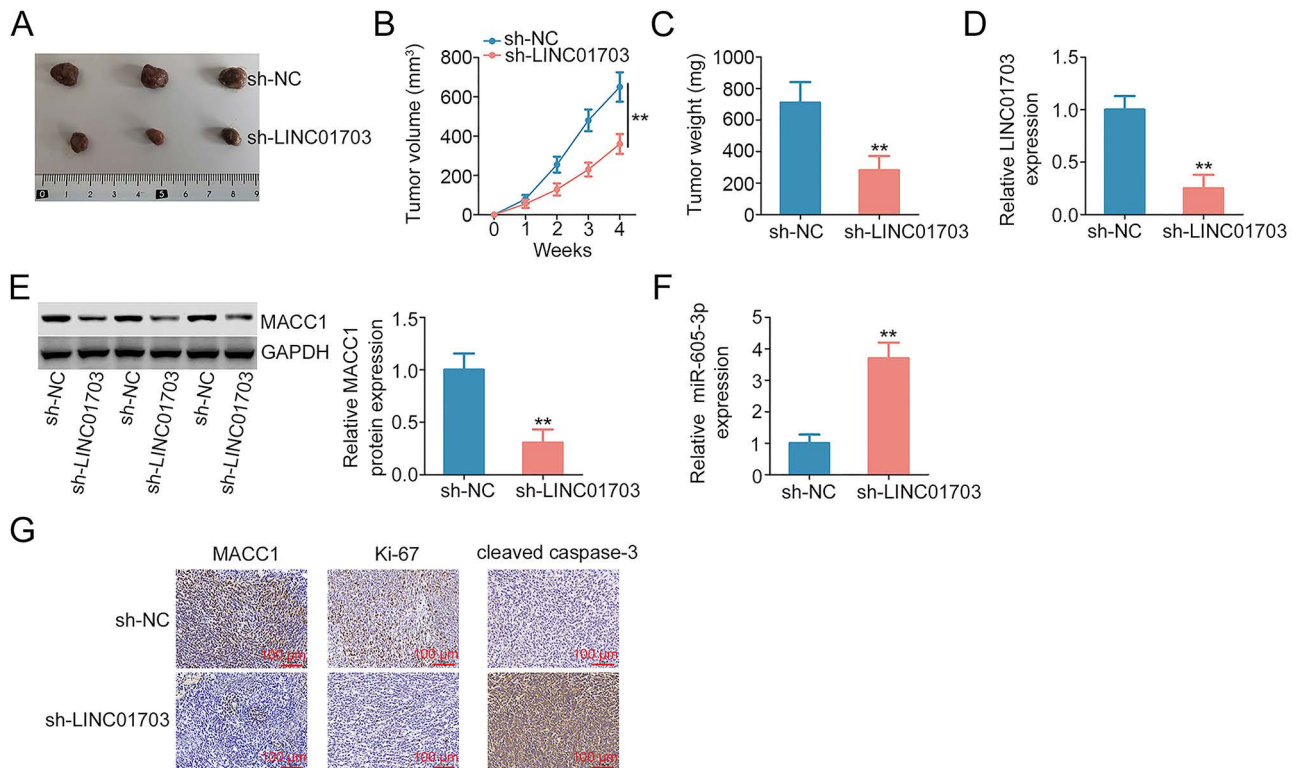


**Figure 8.** The absence of LINC01703 impedes tumor growth in vivo. (A) Macroscopic photographs of xenograft tumors are shown. (B) The growth curve is shown of xenografted tumors in the sh-LINC01703 and negative control shRNA (sh-NC) groups. (C) Xenograft tumors were harvested at 28 days postinjection and then weighed. (D, E) LINC01703 and MACC1 expression in xenograft tumors. (F) miR-605-3p levels in xenograft tumors. (G) Immunohistochemistry experiments were performed to analyze MACC1, Ki-67, and cleaved caspase 3 in tumor xenografts. \*\* $p < 0.01$ .

NSCLC therapy. To date, over 50,000 lncRNAs have been confirmed to exist in the human genome<sup>33</sup>; however, the detailed functions of most lncRNAs are currently unclear. In the current study, we characterized the role of LINC01703 in the malignancy of NSCLC and unraveled the detailed mechanism of action.

LINC01703 was previously confirmed to be an optimal diagnostic biomarker for LUAD<sup>18</sup>. Yet, the expression and specific functions of LINC01703 in NSCLC warrant intensive investigation. In this study, the TCGA database revealed that LINC01703 was overexpressed in NSCLC, which was further proven in our cohort using qRT-PCR. Functional studies revealed that LINC01703 knockdown repressed cell proliferation, colony formation, and motility in vitro, which was accompanied by apoptosis induction. In vivo tumor growth of LINC01703-silenced cells was also inhibited. Accordingly, LINC01703 might be a prospective biomarker for the early diagnosis of NSCLC and offers a novel direction for clinical therapeutic techniques.

Elucidation of the molecular mechanisms mediated by LINC01703 may be helpful in comprehending its role in cancer initiation and progression in depth. lncRNAs implement their regulatory activities by different mechanisms and can dominate gene expression at epigenetic, transcriptional, and posttranscriptional levels<sup>34</sup>. The mechanisms by which lncRNAs function are largely decided by their intracellular location<sup>35</sup>. A myriad of studies have demonstrated that lncRNAs distributed in the cytoplasm can interact with miRNAs as ceRNAs and play important roles in regulating tumorigenic processes<sup>36–38</sup>. lncRNAs can function as ceRNAs or as decoys for specific miRNAs, thus, keeping miRNAs from target genes and consequently upregulating gene expression<sup>39</sup>. Because LINC01703 is localized mainly in the cytoplasm of NSCLC cells, we speculated that cytoplasmic lncRNAs may exacerbate oncogenicity in a ceRNA-dependent manner. Herein, two online databases for lncRNA target prediction were used and indicated a connection between LINC01703 and miR-605-3p. Then, luciferase reporter assays and RIP experiments further proved that LINC01703 acted as a natural molecular sponge for miR-605-3p. Furthermore, we confirmed that miR-605-3p could directly bind and regulate MACC1 in NSCLC cells. Interestingly, miR-605-3p acted as a bridge between LINC01703 and MACC1 in NSCLC cells through similar miRNA response elements. More specifically, MACC1 was downregulated by LINC01703 downregulation but restored by anti-miR-605-3p cotransfection. Thus, a new ceRNA pathway comprising LINC01703, miR-605-3p, and MACC1 was first validated in NSCLC cells.

Recently, the differential expression of miR-605-3p has been reported in many human cancers. miR-605-3p expression is downregulated in hepatocellular

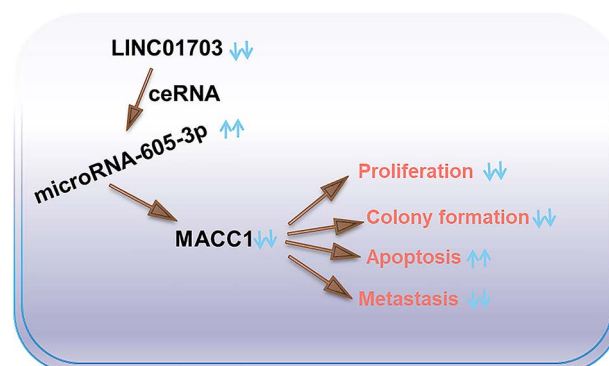


**Figure 9.** The newly identified LINC01703/miR-605-3p/MACC1 pathway in NSCLC.

carcinoma<sup>40</sup>, gastric cancer<sup>41</sup>, prostate cancer<sup>42</sup>, glioma<sup>43</sup>, and bladder cancer<sup>44</sup>. miR-605-3p suppresses tumorigenic properties during cancer onset and progression and participates in the control of cell epithelial–mesenchymal transition, metastasis, growth, apoptosis, and the cell cycle<sup>40–44</sup>. Herein, we also explored the role of miR-605-3p in NSCLC and unraveled its downstream target. Our data showed that miR-605-3p was downregulated in NSCLC and exhibited antioncogenic properties. A further mechanistic investigation identified MACC1 as a downstream effector of miR-605-3p. High expression of MACC1 was reported in NSCLC and was clearly associated with differentiation, the tumor–node–metastasis stage, lymph node metastasis, disease-free survival, and overall survival<sup>45–47</sup>. In addition, MACC1 was verified as an independent biomarker for predicting tumor recurrence and poor prognosis<sup>45,47</sup>. Functionally, activation of MACC1 could exacerbate the aggressiveness of NSCLC and be implicated in the regulation of growth, chemoresistance, metastasis, and cell stemness<sup>48–51</sup>. At the end of our study, rescue experiments were implemented and highlighted that proliferation and colony formation of LINC01703-silenced cells were suppressed, and apoptosis was promoted in cells transfected with si-LINC01703; nevertheless, these regulatory actions were abolished in response to miR-605-3p downregulation or MACC1 overexpression. Therefore, we believe that the carcinogenic roles of LINC01703 in NSCLC cells may occur by modulating the miR-605-3p/MACC1 axis.

In conclusion, LINC01703 sequestered miR-605-3p in NSCLC cells, which, in turn, increased the expression of MACC1, thereby worsening oncogenicity. Hence, our findings may promote the understanding of NSCLC pathogenesis and suggest the therapeutic potential of LINC01703/miR-605-3p/MACC1 (Fig. 9) in the management of NSCLC.

**ACKNOWLEDGMENTS:** This work was financially supported by the Program Funded by the Liaoning Province Education

Administration (No. QN2019003). W.L. and Z.W. designed the study. Z.W., X.Z., X.Z., X.J., and W.L. conducted the cellular experiments. Statistical analysis was implemented by W.L. W.L. and Z.W. wrote the manuscript. The authors declare no conflicts of interest.

## REFERENCES

- Siegel RL, Miller KD, Jemal A. 2020. Cancer statistics, 2020. *CA Cancer J Clin*. 70(1):7–30.
- Bray F, Ferlay J, Soerjomataram I, Siegel RL, Torre LA, Jemal A. 2018. Global cancer statistics 2018: Globocan estimates of incidence and mortality worldwide for 36 cancers in 185 countries. *CA Cancer J Clin*. 68(6):394–424.
- Lemjabbar-Alaoui H, Hassan OU, Yang YW, Buchanan P. 2015. Lung cancer: Biology and treatment options. *Biochim Biophys Acta* 1856(2):189–210.
- Jeong JH, Choi PJ, Yi JH, Jeong SS, Lee KN. 2019. Lymph node metastasis after spontaneous regression of non-small cell lung cancer. *Korean J Thorac Cardiovasc Surg*. 52(2):119–123.
- Yoon SM, Shaikh T, Hallman M. 2017. Therapeutic management options for stage iii non-small cell lung cancer. *World J Clin Oncol*. 8(1):1–20.
- Hirsch FR, Suda K, Wiens J, Bunn PA, Jr. 2016. New and emerging targeted treatments in advanced non-small-cell lung cancer. *Lancet* 388(10048):1012–1024.
- Mattick JS, Makunin IV. 2006. Non-coding RNA. *Hum Mol Genet*. 15(Spec No 1):R17–29.
- Sun M, Kraus WL. 2015. From discovery to function: The expanding roles of long noncoding RNAs in physiology and disease. *Endocr Rev*. 36(1):25–64.
- Bhan A, Soleimani M, Mandal SS. 2017. Long non-coding RNA and cancer: A new paradigm. *Cancer Res*. 77(15):3965–3981.
- Liu R, Wang X, Shen Y, He A. 2021. Long non-coding RNA-based glycolysis-targeted cancer therapy: Feasibility, progression and limitations. *Mol Biol Rep*. 48(3):2713–2727.
- Chen J, Wang R, Zhang K, Chen LB. 2014. Long non-coding RNAs in non-small cell lung cancer as biomarkers and therapeutic targets. *J Cell Mol Med*. 18(12):2425–2436.
- He L, Hannon GJ. 2004. MicroRNAs: Small RNAs with a big role in gene regulation. *Nat Rev Genet*. 5(7):522–531.
- Hammond SM. 2015. An overview of microRNAs. *Adv Drug Deliv Rev*. 87:3–14.
- He B, Zhao Z, Cai Q, Zhang Y, Zhang P, Shi S, Xie H, Peng X, Yin W, Tao Y, Wang X. 2020. Mirna-based biomarkers, therapies, and resistance in cancer. *Int J Biol Sci*. 16(14):2628–2647.
- Guo T, Li J, Zhang L, Hou W, Wang R, Zhang J, Gao P. 2019. Multidimensional communication of microRNAs and long non-coding RNAs in lung cancer. *J Cancer Res Clin Oncol*. 145(1):31–48.
- Tang LX, Chen GH, Li H, He P, Zhang Y, Xu XW. 2018. Long non-coding RNA OGF1P1 regulates LYPD3 expression by sponging mir-124-3p and promotes non-small cell lung cancer progression. *Biochem Biophys Res Commun*. 505(2):578–585.
- Huang YF, Zhang Y, Fu X. 2021. Long non-coding RNA DANCR promoted non-small cell lung cancer cells metastasis via modulating of mir-1225-3p/ErbB2 signal. *Eur Rev Med Pharmacol Sci*. 25(2):758–769.
- Wang Y, Fu J, Wang Z, Lv Z, Fan Z, Lei T. 2019. Screening key lncRNAs for human lung adenocarcinoma based on machine learning and weighted gene co-expression network analysis. *Cancer Biomark*. 25(4):313–324.
- Livak KJ, Schmittgen TD. 2001. Analysis of relative gene expression data using real-time quantitative pcr and the 2(-delta delta c(t)) method. *Methods* 25(4):402–408.
- Ding L, Fang Y, Li Y, Hu Q, Ai M, Deng K, Huang X, Xin H. 2021. AIMP3 inhibits cell growth and metastasis of lung adenocarcinoma through activating a miR-96-5p-AIMP3-p53 axis. *J Cell Mol Med*. 25(6):3019–3030.
- Wang D, Zhang S, Zhao M, Chen F. 2020. LncRNA MALAT1 accelerates non-small cell lung cancer progression via regulating mir-185-5p/MDM4 axis. *Cancer Med*. 9(23):9138–9149.
- Han J, Hu J, Sun F, Bian H, Tang B, Fang X. 2021. MicroRNA-20a-5p suppresses tumor angiogenesis of non-small cell lung cancer through RRM2-mediated PI3K/Akt signaling pathway. *Mol Cell Biochem*. 476(2):689–698.
- Liu Y, Xu B, Liu M, Qiao H, Zhang S, Qiu J, Ying X. 2021. Long non-coding RNA SNHG25 promotes epithelial ovarian cancer progression by up-regulating COMP. *J Cancer* 12(6):1660–1668.
- Yao Q, Chen T. 2020. LINC01128 regulates the development of osteosarcoma by sponging mir-299-3p to mediate MMP2 expression and activating Wnt/beta-catenin signaling pathway. *J Cell Mol Med*. 24(24):14293–14305.
- Bai Y, Lang L, Zhao W, Niu R. 2019. Long non-coding RNA HOXA11-as promotes non-small cell lung cancer tumorigenesis through microRNA-148a-3p/DNMT1 regulatory axis. *Onco Targets Ther*. 12:11195–11206.
- Raissi V, Zibaei M, Raiesi O, Samani Z, Yarahmadi M, Etemadi S, Istiqomah A, Alizadeh Z, Shadabi S, Sohrabi N, Ibrahim A. 2021. Parasite-derived microRNAs as a diagnostic biomarker: Potential roles, characteristics, and limitations. *J Parasit Dis*. 45(2):546–556.
- Chen Y, Li Z, Chen X, Zhang S. 2021. Long non-coding RNAs: From disease code to drug role. *Acta Pharm Sin B* 11(2):340–354.
- Rodriguez M, Ajona D, Seijo LM, Sanz J, Valencia K, Corral J, Mesa-Guzman M, Pio R, Calvo A, Lozano MD, Zulueta JJ, Montuenga LM. 2021. Molecular biomarkers in early stage lung cancer. *Transl Lung Cancer Res*. 10(2):1165–1185.
- Sanchez Calle A, Kawamura Y, Yamamoto Y, Takeshita F, Ochiya T. 2018. Emerging roles of long non-coding RNA in cancer. *Cancer Sci*. 109(7):2093–2100.
- Li G, Li X, Yuan C, Zhou C, Li X, Li J, Guo B. 2021. Long non-coding RNA JPX contributes to tumorigenesis by regulating mir-5195-3p/VEGFA in non-small cell lung cancer. *Cancer Manag Res*. 13:1477–1489.
- Zeng SHG, Xie JH, Zeng QY, Dai SHH, Wang Y, Wan XM, Liu JCH. 2021. lncRNA PVT1 promotes metastasis of non-small cell lung cancer through EZH2-mediated activation of hippo/NOTCH1 signaling pathways. *Cell J*. 23(1):21–31.
- Wei MM, Zhou GB. 2016. Long non-coding RNAs and their roles in non-small-cell lung cancer. *Genomics Proteomics Bioinformatics* 14(5):280–288.
- Xu J, Bai J, Zhang X, Lv Y, Gong Y, Liu L, Zhao H, Yu F, Ping Y, Zhang G, Lan Y, Xiao Y, Li X. 2017. A comprehensive overview of lncRNA annotation resources. *Brief Bioinform*. 18(2):236–249.
- Liu W, Ma R, Yuan Y. 2017. Post-transcriptional regulation of genes related to biological behaviors of gastric cancer by long noncoding RNAs and microRNAs. *J Cancer*. 8(19):4141–4154.

35. Lu CW, Zhou DD, Xie T, Hao JL, Pant OP, Lu CB, Liu XF. 2018. HOXA11 antisense long noncoding RNA (HOXA11-AS): A promising lncRNA in human cancers. *Cancer Med.* 7(8):3792–3799.
36. Wang X, Yu X, Long X, Pu Q. 2021. MIR205 host gene (MIR205HG) drives osteosarcoma metastasis via regulating the microRNA 2114-3p (miR-2114-3p)/twist family bHLH transcription factor 2 (TWIST2) axis. *Bioengineered* 12(1):1576–1586.
37. Guan B, Ma J, Yang Z, Yu F, Yao J. 2021. LncRNA NCK1-AS1 exerts oncogenic property in gastric cancer by targeting the mir-22-3p/BCL9 axis to activate the Wnt/ $\beta$ -catenin signaling. *Environ Toxicol.* 36(8):1640–1653.
38. Chen Y, Zhang R. 2021. Long non-coding RNAAL139002.1 promotes gastric cancer development by sponging microRNA-490-3p to regulate hepatitis a virus cellular receptor 1 expression. *Bioengineered* 12(1):1927–1938.
39. Lin W, Liu H, Tang Y, Wei Y, Wei W, Zhang L, Chen J. 2021. The development and controversy of competitive endogenous RNA hypothesis in non-coding genes. *Mol Cell Biochem.* 476(1):109–123.
40. Hu YL, Feng Y, Chen YY, Liu JZ, Su Y, Li P, Huang H, Mao QS, Xue WJ. 2020. *SNHG16/miR-605-3p/TRAF6/NF- $\kappa$ B* feedback loop regulates hepatocellular carcinoma metastasis. *J Cell Mol Med.* 24(13):7637–7651.
41. Su YZ, Cui MF, Du J, Song B. 2020. LncRNA DCST1-AS1 regulated cell proliferation, migration, invasion and apoptosis in gastric cancer by targeting miR-605-3p. *Eur Rev Med Pharmacol Sci.* 24(3): 158–1167.
42. Pan MZ, Song YL, Gao F. 2019. MiR-605-3p inhibits malignant progression of prostate cancer by up-regulating EZH2. *Eur Rev Med Pharmacol Sci.* 23(20):8795–8805.
43. Liu N, Hu G, Wang H, Wang Y, Guo Z. 2019. LncRNA BLACAT1 regulates VASP expression via binding to miR-605-3p and promotes glioma development. *J Cell Physiol.* 234(12):22144–22152.
44. Zeng Z, Zhou W, Duan L, Zhang J, Lu X, Jin L, Yu Y. 2019. Circular RNA circ-VANGL1 as a competing endogenous RNA contributes to bladder cancer progression by regulating miR-605-3p/VANGL1 pathway. *J Cell Physiol.* 234(4):3887–3896.
45. Shimokawa H, Uramoto H, Onitsuka T, Chundong G, Hanagiri T, Oyama T, Yasumoto K. 2011. Overexpression of MACC1 mRNA in lung adenocarcinoma is associated with postoperative recurrence. *J Thorac Cardiovasc Surg.* 141(4):895–898.
46. Hu X, Fu X, Wen S, Zou X, Liu Y. 2012. [Prognostic value of MACC1 and c-met expressions in non-small cell lung cancer]. *Zhongguo Fei Ai Za Zhi.* 15(7):399–403.
47. Chundong G, Uramoto H, Onitsuka T, Shimokawa H, Iwanami T, Nakagawa M, Oyama T, Tanaka F. 2011. Molecular diagnosis of MACC1 status in lung adenocarcinoma by immunohistochemical analysis. *Anticancer Res.* 31(4):1141–1145.
48. Zhang Q, Zhang B, Sun L, Yan Q, Zhang Y, Zhang Z, Su Y, Wang C. 2018. Cisplatin resistance in lung cancer is mediated by MACC1 expression through PI3K/Akt signaling pathway activation. *Acta Biochim Biophys Sin (Shanghai)* 50(8):748–756.
49. Li Z, Guo T, Fang L, Li N, Wang X, Wang P, Zhao S, Li F, Cui Y, Shu X, Zhao L, Li J, Gu C. 2019. MACC1 overexpression in carcinoma-associated fibroblasts induces the invasion of lung adenocarcinoma cells via paracrine signaling. *Int J Oncol.* 54(4):1367–1375.
50. Guo L, Ou S, Ma X, Zhang S, Lai Y. 2018. MACC1 silencing inhibits cell proliferation and induces cell apoptosis of lung adenocarcinoma cells through the  $\beta$ -catenin pathway. *Neoplasma* 65(4):552–560.
51. Wang X, Yu X, Wei W, Liu Y. 2020. Long noncoding RNA MACC1-AS1 promotes the stemness of non-small cell lung cancer cells through promoting UPF1-mediated destabilization of LATS1/2. *Environ Toxicol.* 35(9):998–1006.